Cytokine 120 (2019) 155–164

Contents lists available at ScienceDirect

Cytokine

journal homepage: www.elsevier.com/locate/cytokine

Resistin induces breast cancer cells epithelial to mesenchymal transition (EMT) and stemness through both adenylyl cyclase-associated protein 1 (CAP1)-dependent and CAP1-independent mechanisms

Dimiter Avtanski[a,b,c,*], Anabel Garcia[a], Beatriz Caraballo[a], Priyanthan Thangeswaran[a], Sela Marin[a], Julianna Bianco[a], Aaron Lavi[a], Leonid Poretsky[a,b,c]

[a] Friedman Diabetes Institute at Lenox Hill Hospital, Northwell Health, New York, NY, USA
[b] The Feinstein Institute for Medical Research, Northwell Health, Manhasset, NY, USA
[c] Donald and Barbara Zucker School of Medicine at Hofstra/Northwell, Hempstead, NY, USA

ARTICLE INFO

Keywords:
Resistin
CAP1
Breast cancer
EMT
CSC

ABSTRACT

Breast cancer incidence and metastasis in postmenopausal women are known to associate with obesity, but the molecular mechanisms behind this association are largely unknown. We investigated the effect of adipokine resistin on epithelial to mesenchymal transition (EMT) and stemness in breast cancer cells *in vitro*. Previous reports demonstrated that the inflammatory actions of resistin are mediated by the adenylyl cyclase-associated protein 1 (CAP1), which serves as its receptor. As a model for our study, we used MCF-7 and MDA-MB-231 breast cancer and MCF-10A breast epithelial cells. We showed that in MCF-7 cells resistin increases the migration of MCF-7 and MDA-MB-231 cells and induces the formation of cellular protrusions through reorganization of F-actin filaments. Resistin upregulated the expression of mesenchymal markers involved in EMT (SNAIL, SLUG, ZEB1, TWIST1, fibronectin, and vimentin), and downregulated those of epithelial markers (E-cadherin and claudin-1). Resistin also potentiated the nuclear translocation of SNAIL protein, indicating initiation of EMT reprogramming. We further induced EMT in non-carcinogenic breast epithelial MCF-10A cells demonstrating that the effects of resistin on EMT were not breast cancer cell specific. In order to assess whether resistin-induced EMT depends on CAP1, we used siRNA approach to silence CAP1 gene in MCF-7 cells. Results demonstrated that when CAP1 was silenced, the induction of SNAIL, ZEB1 and vimentin expression by resistin as well as SNAIL and ZEB1 nuclear translocation, were abolished. Additionally, CAP1 silencing resulted in a suppression of MCF-7 cells migration. We performed quantitative PCR array profiling the expression of 84 genes related to cancer stem cells (CSC), pluripotency and metastasis and selected a set of genes (ALDH1A1, ITGA4, LIN28B, SMO, KLF17, PTPRC, PROM1, SIRT1, and PECAM1) that were modulated by resistin. Further experiments demonstrated that the effect of resistin on the expression of some of these genes (PROM1, PTPRC, KLF17, SIRT1, and PECAM1) was also dependent on CAP1. Our results demonstrate that resistin promotes the metastatic potential of breast cancer cells by inducing EMT and stemness and some of these effects are mediated by CAP1.

1. Introduction

Obesity is associated with the development and progression of multiple types of cancer including breast cancer in postmenopausal women and men [1–4]. Obesity currently represents a worldwide epidemic affecting more than 650 million people [5], and breast cancer is the second leading cancer among women, accounting for nearly 1 in 3 diagnosed cancers or 16% of all female cancers [6]. Although genetic predisposition appears to be the main factor for breast cancer initiation and progression, breast cancer metastasis in postmenopausal women associates with obesity. High caloric intake significantly increases the development of mammary tumors in rats and mice, and caloric restriction decreases cancer incidence and tumor growth [7–9]. In human, obesity is associated with increased risk of cancer recurrence and higher mortality rate [10]. The effects of obesity on breast cancer are attributed, at least in part, to the excessive amount of peripheral fat, which in postmenopausal women is the primary source of estrogens [11].

Abbreviations: EMT, epithelial to mesenchymal transition; CAP1, adenylyl cyclase-associated protein 1; CSC, cancer stem cell

* Corresponding author at: Friedman Diabetes Institute, Northwell Health, 110 E 59th Street, Suite 8B, Rm 837, New York, NY 10022, USA.
E-mail address: davtanski@northwell.edu (D. Avtanski).

https://doi.org/10.1016/j.cyto.2019.04.016
Received 9 January 2019; Received in revised form 21 March 2019; Accepted 22 April 2019
Available online 11 May 2019
1043-4666/

One of the key steps in metastasis is the epithelial to mesenchymal transition (EMT), a process in which cancer cells lose their epithelial characteristics and gain mesenchymal-like features, thus increasing cellular migration and invasion. In the context of cancer, EMT induces the acquisition of cells with stem cell (CSC) characteristics, and the CSC are believed to have the ability to initiate new tumors [12].

Resistin is an adipokine produced by adipocytes and macrophages in the white adipose tissue (WAT) and it plays a role in inflammation and insulin resistance [13,14]. In humans, circulating levels of resistin increase with adiposity and are reduced after exercise [15–21]. Pre-operative plasma levels of resistin were found to be predictive of the extent of weight loss after gastric bypass surgery [22]. Various mouse models of obesity (diet-induced obese [DIO] C57Bl/6J, high fat-fed tumor necrosis factor alpha-deficient $(TNF\alpha)^{-/-}$ and brown adipose tissue [BAT]-deficient uncoupling protein-diphtheria toxin A chain [UCP1-DTA]) are characterized by higher blood resistin levels [23]. Additionally, circulating concentrations of resistin are positively associated with the risk of breast cancer initiation [24]. Mean serum resistin levels are significantly higher in patients with breast cancer lesions and correlate with tumor and inflammatory markers, cancer stage, tumor size, grade and lymph node invasion [25,26]. There is a significant association of resistin with cancer progression and increased metastatic potential of cancer cells [27]. In MDA-MB-231 breast cancer cells, resistin was found to promote metastasis through activation of ezrin, radixin and moesin (ERM protein family), which links F-actin to cell membrane proteins following phosphorylation [28]. Resistin was found to confer CSC-like characteristics in MDA-MB-231 and MDA-MB-468 breast cancer cells by involving STAT3 [29]. In a recent study, resistin was shown to induce acquisition of mesenchymal phenotype and CSC-like features in breast cancer cells through activation of toll-like receptor 4 (TLR4)/NF-κB/STAT3 signaling pathway [30]. Resistin also enhanced the mammosphere formation in MCF-7, T47D, and HS-578T breast cancer cells concomitantly with elevation of SOX2, NANOG, and OCT4 (POU5F1) protein expression [30]. In the same study, it was found that incubation of MCF-7 and T47D cells with resistin (50 ng/ml) for 10 days increased the proportion of $CD44^{high}/CD24^{-/low}$ cells [30].

Monocyte inflammatory actions of resistin are mediated by adenylyl cyclase-associated protein 1 (CAP1) which serves as receptor for resistin [31,32]. CAP was first identified in *Saccharomyces cerevisiae* as a component of the adenylate cyclase complex CYR1P [33]. CAP consists of six highly-conserved structural domains in their N- and C-terminus, and Src homology 3 (SH3) binding domain [34]. The N-termini binds to adenylyl cyclase and plays a role in Ras signaling [35], while the C-termini binds to G-actin and affects microfilament reorganization [36]. The internal part of CAP contains the WASP2 domain (WH2), which associates with cytoskeleton element polymerization and remodeling [35]. CAP1 homolog possess various functions [37], including directly to regulate the cofilin-1 protein [38] thus exerting effects on actin fiber reorganization and cell migration [39]. Upregulated expression of CAP1 was found to closely correlate with tumor metastasis parameters in hepatocellular carcinoma (HCC), and univariate analyses showed that CAP1 could be used as a prognostic marker for patients' survival [40]. In the same study, knocking-down CAP1 expression by using short interfering RNA (siRNA) let to impaired HCC migration. Silencing of CAP1 and/or TLR4 in MiaPaCa-2 and SW1990 human pancreatic cancer cells resulted in a marked reduction in resistin-induced proliferation, migration, invasion, and cell cycle [26]. It was demonstrated [41] that resistin and CAP1 gene polymorphisms and expression may be used as potential biomarkers for breast cancer risk.

In this study, we hypothesized that resistin increases breast cancer metastasis potential through induction of EMT and acquisition of CSC-like properties in breast cancer cells, and that these effects may be associated with CAP1. We selected two breast cancer cell lines, MCF-7 (low-metastatic) and MDA-MB-231 (high-metastatic) as well as non-tumorigenic breast epithelial MCF-10A cell lines as *in vitro* models for our experiments.

2. Materials and methods

2.1. Reagents

Human recombinant resistin (Cat. # PF-138) was purchased from Calbiochem® (EMD Millipore Corp., Temecula, CA, USA). The lyophilized form was reconstituted with water to a concentration of 100 μg/ml and further to a series of dilutions of 8.3, 12.5, 25, and 50 μg/ml, which were used for cell treatment.

2.2. Cell lines and reagents

Human breast cancer MCF-7, MDA-MB-231, and MCF-10A cells were purchased from American Type Culture Collection (ATCC) (Cat. ## HTB-22, HTB-26, and CRL-10317). MCF-7 and MDA-MB-231 cells were grown in Dulbecco's Modified Eagle's Medium (DMEM) (Cat. # 10-013-CF, Corning Inc.) supplemented with 10% FBS (Cat. # 1500-500, VWR International) and 1x Antibiotic/Antimycotic Solution (Cat. # 30-004-CI, Corning, Inc.). MCF-10 cells were grown in HuMEC Ready Medium kit (Cat. # 12-752-010, Gibco™, Thermo Fisher Scientific) containing HuMEC Basal Serum Free Medium, HuMEC Supplement and Bovine Pituitary Extract (BPE), which was additionally supplemented with 10% FBS and 1x Antibiotic/Antimycotic Solution.

2.3. Scratch migration wound healing assay

For scratch migration wound healing assay, the cells were seeded in 6-well plates in a 100% confluent monolayer. One day after seeding, a scratch was made by using a sterile pipette tip. Plates were washed one time with fresh medium and then the medium was replaced with complete medium with or without resistin (12.5 or 25 ng/ml). Series of phase-contrast pictures at 10× magnification were taken before and at 3, 6, 15, 18, and 24 h after treatment by using EVOS Fl Auto Cell Imaging System (Thermo Fisher Scientific). Experiments were repeated at least three times in duplicates. For each image, scratch width was measured in 4 different areas in 4 separate images as the data for each time-point (3, 6, 15, 18, and 24 h) were normalized to 0 h for each well individually. The data from the control wells for each time point were then normalized to 100%, and the data for resistin treatment were presented as percent compared to the corresponding control for each time-point.

2.4. Transwell migration assay

Transwell migration assays were performed by using HTC Transwell® 24-well plates (Cat. # 3398, Costar) with 3 μm pore size. All experiments were performed three times in duplicates. Images were taken by using EVOS XL Cell Imaging System (Life Technologies) at 10× magnification. Data analyses were performed by using 4 images per well and data were presented as percentage of migrated cells of each treatment compared to control (± SEM).

2.5. Quantitative RT-PCR analyses

After experiments were performed, cells were washed twice with sterile PBS and total RNA was extracted by using TRIzol™ reagent (Ambion, Thermo Fisher Scientific) and chloroform and precipitated with iso-propanol (VWR International). The precipitated RNA was washed once with 70% ethanol, air-dried and resuspended in sterile, nuclease-free water. After resuspension, the samples were incubated at 65 °C for 10 min and stored at −86 °C for further use. For RT conversion, the initial RNA concentration was determined by using NanoDrop™ One Microvolume UV–Vis Spectrophotometer (Thermo Fisher Scientific). Samples were then normalized to 1 mg/ml RNA and RT reaction was performed by using qScript cDNA Synthesis Kit (Quanta Bio) and SimpliAmp Thermal Cycler (Applied Biosystems,

Thermo Fisher Scientific). Quantitative PCR analyses were performed by using PowerUp SYBR Green Master Mix and QuantStudio 3 Real-Time PCR System (Applied Biosystems, Thermo Fisher Scientific). Information about the primer sequences and annealing temperature is provided in Supplemental Table 1. Each experiment was performed 4 to 6 times in duplicates, and for PCR analysis each sample was analyzed twice.

2.6. Western blot analyses

Whole cellular protein was extracted by using Pierce™ RIPA Lysis Buffer (Cat. # 89901, Thermo Fisher Scientific), supplemented with protease inhibitor cocktail (Mammalian ProteaseArrest, Cat. # 786-331, G-Biosciences) and phosphatase inhibitors (PhosphataseArrest™, Cat. # 786-450, G-Biosciences). Cytoplasmic and nuclear protein fractures were extracted by using Nuclear & Cytoplasmic Extraction Kit (Cat. # 786-182, G Biosciences®) following manufacturer's protocol. Protein concentrations were quantified by using Pierce™ BCA Protein Assay Kit (Cat. # 23225, Thermo Fisher Scientific), BioTek® plate reader and Gen5™ data analysis software (BioTek®). Normalized to 1 mg protein extracts were separated by polyacrylamide gel electrophoresis (SDS-PAGE) and transferred onto nitrocellulose membranes (Amersham, GE Healthcare). Membranes were blotted with SNAIL (C15D3) Rabbit mAb (Cat. # 3879), SLUG (C19G7) Rabbit mAb (Cat. # 9585), TCF8/ZEB1 (D80D3) Rabbit mAb (Cat. # 3396), Vimentin (D21H3) XP Rabbit mAb (Cat. # 5741), N-cadherin (D4R1H) XP Rabbit mAb (Cat. # 13116), E-cadherin (24E10) Rabbit mAb (Cat. # 3195), Claudin-1 (D5H1D) XP Rabbit mAb (Cat. # 13255), CAP1 (D2K3J) Rabbit mAb (Cat. # 47055), GAPDH (14C10) Rabbit mAb (Cat. # 2118) (Cell Signaling Technology), β Tubulin (D-10) mAb (Cat. # sc-5274), and Lamin B1 (B-10) mAb (Cat. # sc-374015) (Santa Cruz Biotechnology) primary antibodies and Pierce™ Goat Anti-Rabbit and Anti-Mouse Horseradish Peroxidase Conjugated Secondary Antibodies (Cat. ## 31460 and 31430, Thermo Fisher Scientific). Protein bands were visualized by using SuperSignal West Pico Chemiluminescent Substrate (Cat. # 34580, Cell Signaling Technology) and MyECL™ imager (Thermo Fisher Scientific). All Western blot experiments were performed 3 times. Densitometry analyses were performed with ImageJ software (National Institutes of Health) and protein expression levels were presented as percentage difference compared to control (± SEM).

2.7. Immunofluorescence microscopy

For immunofluorescence microscopy, cells were grown in Thermo Scientific™ Nunc™ Lab-Tek™ II Chamber Slide System (Thermo Fisher Scientific). After the experiment, cells were washed one-time with sterile PBS and processed for immunofluorescence staining following Immunofluorescence General Protocol and using reagents from Cell Signaling Technology. Specimens were initially fixed in 4% folmaldehyde (diluted in PBS), then blocked in blocking buffer (containing PBS/5% normal serum/0.3% Triton™ X-100) for 60 min and incubated overnight at room temperature with primary antibodies diluted 1:100 in antibody dilution buffer (PBS/1% BSA/0.3% Triton™ X-100). The following primary antibodies were used: SNAIL (C1503) Rabbit mAB (Cat. # 3897), TCF8/ZEB1 (D80D3) Rabbit mAb (Cat. # 3396), E-cadherin (24E10) Rabbit mAb (Cat. # 3195), and Claudin-1 (D5H1D) Rabbit mAb (Cat. # 13255). Specimens were then incubated with Anti-Rabbit IgG (H + L), $F(ab')_2$ Alexa Fluor® 488 and 555 secondary antibodies (Cat. ## 4412 and 4413, Cell Signaling Technology) diluted 1:500 in antibody dilution buffer for two hours at room temperature. The slides were coverslip with ProLong Gold Antifade Reagent with DAPI (Cat. # 8961) and left to dry overnight in the dark at room temperature. Staining with phalloidin was performed by using Alexa Fluor® 555 Phalloidin (Cat. # 8953). Microscopy was performed using EVOS Fl Auto Cell Imaging System (Thermo Fisher Scientific) equipped with GFP (excitation 470/22 nm; emission 525/50 nm), RFP (excitation 531/40 nm; emission 593/40 nm) and DAPI (excitation 357/44 nm; emission 447/60 nm) EVOS LED cubes at 100× magnification.

2.8. siRNA transfections

For transfections, 0.25–1 × 10^6 MCF-7 cells were seeded in 6-well plates 24 h prior to each experiment to achieve 60–80% confluency. Transfection was performed using UltraMEM™ Reduced Serum Medium (Lonza Group AG), Lipofectamine® RNAiMAX (Cat. # 13778150) and Silencer® Select pre-designed CAP1 siRNA (Cat. # 4392420, Assay ID s20547, Thermo Fisher Scientific). Cells were transfected with 15 nM CAP1 or negative control siRNA for 4 h. After incubation, the medium was replaced with complete growing medium in which the cells were grown overnight. On the following day the cells were treated with resistin (12.5 ng/ml) for 6 h.

2.9. Quantitative PCR array

Total RNA from MCF-7 cells was extracted by using TRIzol®/chloroform/isopropanol method. RNA extracts were normalized to 0.5 μg/ml and reverse transcribed by using qScript cDNA SuperMix (Quanta Biosciences) and SimpliAmp™ Thermal Cycler. Human Cancer Stem Cells RT^2 Profiler PCR array (Cat. # PAHS-176Z, QIAGEN Sciences) using RT^2 SYBR Green ROX qPCR Mastermix (Cat. # 330520, QIAGEN Sciences) and QuantStudio™ 3 Real-Time PCR System (Applied Biosystems, Thermo Fisher Scientific) was used to profile the expression of 84 genes linked to cancer stem cells. The complete list of genes included in this assay is presented in Supplemental Table 13. Data were analyzed using PCR Array Data Analysis online software (QIAGEN Sciences) and $\Delta\Delta Ct$ method to evaluate the relative quantification. A set of controls was used to assess the reverse transcription performance, genomic DNA contamination, and PCR performance.

2.10. Statistical analyses

Quantitative RT-PCR analyses data were based on 4–6 separate experiments, as each experimental condition was set up in duplicates, and each sample was analyzed in duplicates. Densitometry analysis of the Western blot data was based on 3 separate experiments. Statistical analysis was carried out using GraphPad Prism 7 software (GraphPad Software). Data were analyzed using Student's t test and two-tailed distribution or ANOVA. Results are expressed as mean ± SEM and are considered statistically significant if $p < 0.05$.

3. Results

3.1. Optimization of resistin treatment

Initially, in order to optimize the experimental conditions, MCF-7 and MDA-MB-231 cells were treated with resistin at concentrations of 8.3, 12.5, 25, and 50 ng/ml for 6 and 24 h and the expression of SOCS3 (a known target of resistin) was measured by using qRT-PCR. As demonstrated in Fig. 1 and Table 1 in Ref. [42], resistin significantly upregulated SOCS3 mRNA levels. Maximum effect was achieved at concentration of 12.5 ng/ml for 6 h by up to 1.8-fold in MCF-7 and 2.2-fold in MDA-MB-231 cells, compared to non-treated cells (control). Additionally, we performed cell counts while using different treatment conditions (data not shown). Results from these experiments did not show any significant effect on MCF-7 and MDA-MB-231 cell proliferation or death while using resistin in concentrations between 12.5 and 25 ng/ml. Based on these results, we continued our further experiments using resistin concentrations of 12.5 and 25 ng/ml.

3.2. Resistin increases cell migration and induces breast cancer cell motility

To examine the effect of resistin on breast cancer cell motility, MCF-

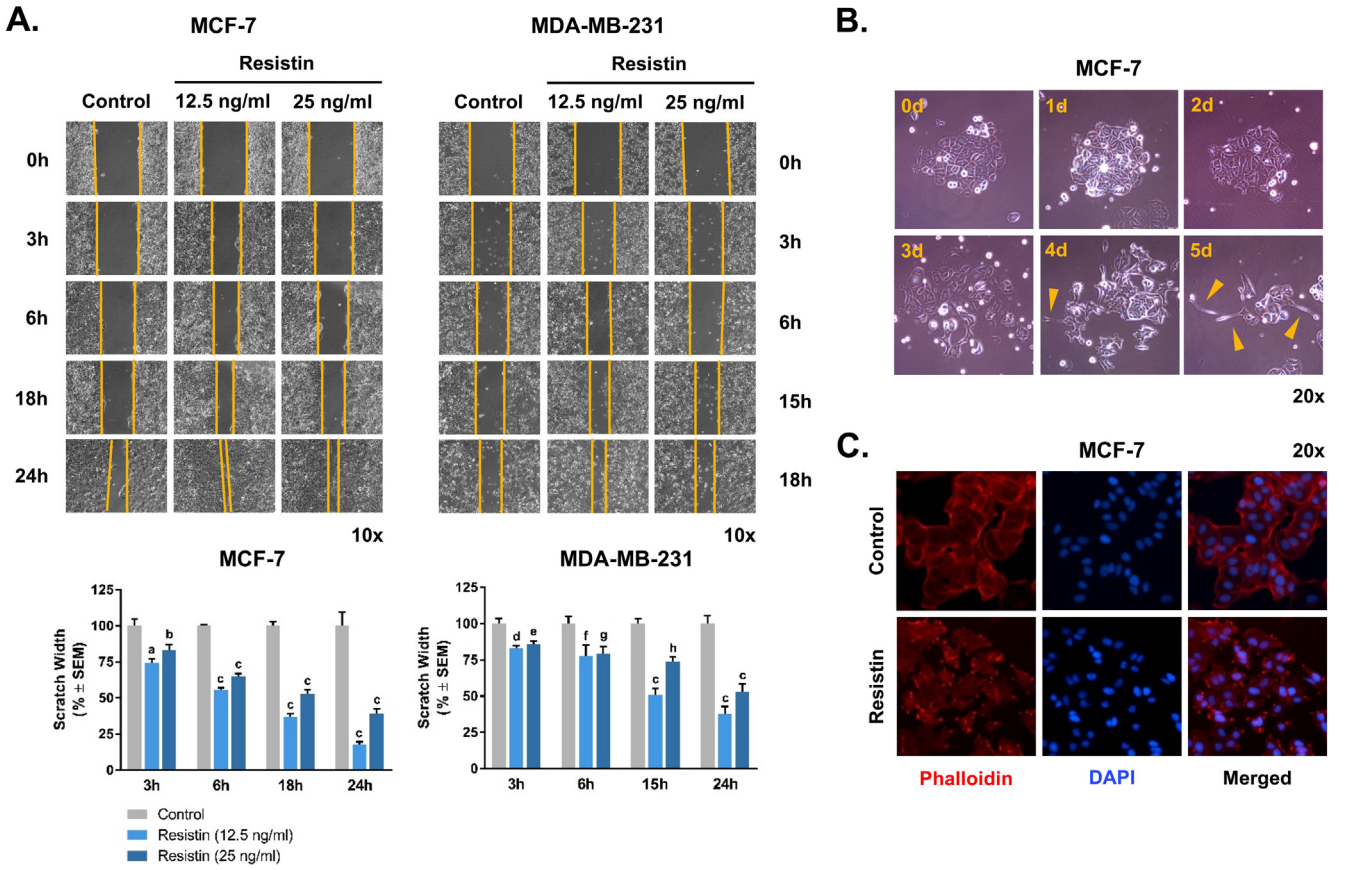

Fig. 1. Resistin increases cell migration and induces the motility of breast cancer cells. A. MCF-7 and MDA-MB-231 cells were subjected to scratch migration wound healing assay. Cells were treated with resistin (12.5 and 25 ng/ml) for up to 24 h. Migration rate was evaluated by measuring the gap width in 4 areas in 4 separate images and normalized to 0 h of treatment. Data are presented as fold change of resistin treatment compared to non-treatment control cells. Scratch width and *p* values are listed in Supplemental Table 2). B. MCF-7 cells were treated with resistin (12.5 ng/ml) for up to 5 days. Phase-contrast images were taken before and once every day after treatment. Arrows indicate the formation of cellular protrusions. Magnification 20×. C. Immunofluorescence imaging of MCF-7 cells stained with phalloidin (red) demonstrating reorganization of F-actin cellular fibers. Nuclei were visualized by DAPI (blue). Magnification 20×. (For interpretation of the references to colour in this figure legend, the reader is referred to the web version of this article.)

7 and MDA-MB-231 cells were subjected to scratch migration wound healing assay. Cells were treated with resistin (12.5 and 25 ng/ml) and cellular migration was compared to that of non-treated control cells. Resistin significantly increased MCF-7 and MDA-MB-231 cell motility after 6 h of treatment until completion of the experiment by 24 h (Fig. 1A and Supplemental Table 2). We also investigated the effect of resistin treatment on MCF-7 cell morphology by treating these cells with resistin (12.5 ng/ml) for up to 5 days. Three days after initiation of treatment, we detected a separation of single cells from the cellular clusters, and by five days after treatment a formation of cellular protrusions (filopodia and lamellipodia) (Fig. 1B). Immunofluorescence microscopy using phalloidin staining revealed reorganization of the F-actin cellular fibers to the newly formed cellular protrusions (Fig. 1C and Supplemental Fig. 1).

3.3. Resistin induces EMT in breast cancer cells

To investigate whether resistin modulates breast cancer cell motility through induction of EMT, we treated breast cancer cells with resistin and evaluated the expression of various epithelial and mesenchymal markers. We carried out a concentration-response and time-dependent experiment, using MDA-MB-231 cells testing different concentrations of resistin (12.5, 25 and 50 ng/ml) for 6 and 24 h and found that the best effect was achieved at concentration of 12.5 ng/ml (see Fig. 2 and Table 2 in Ref. [42]). We further performed experiments using MCF-7 and MDA-MB-231 cells treated with resistin (12.5 ng/ml) for 6 and 24 h. The results showed that resistin upregulated mRNA levels of transcription factors SNAIL (*s.* SNAI1), SLUG (*s.* SNAI2), ZEB1 (*s.* TCF8), and TWIST1 and those of the mesenchymal markers fibronectin and vimentin (Fig. 2A and Supplemental Table 3). Western blot analyses demonstrated that resistin upregulated protein expression levels of SNAIL and vimentin mesenchymal markers, while downregulating protein expression of the epithelial markers E-cadherin and claudin-1 (Fig. 2B and Table 3 in Ref. [42]). Immunofluorescence microscopy confirmed a decreased peripheral staining for E-cadherin and claudin-1 proteins after resistin treatment (Fig. 1C). Immunofluorescence microscopy and Western blot analyses where sub-cellular fractions of cytoplasmic and nuclear proteins were extracted separately revealed that in MCF-7 cells resistin not only increased the expression of SNAIL and ZEB1 proteins, but also induced their nuclear translocation (Fig. 2D and E, and Table 4 in Ref. [42]).

3.4. Resistin induces EMT in non-carcinogenic breast epithelial cells

To examine whether the observed effects of resistin are limited to breast cancer cells, we utilized non-carcinogenic breast epithelial MCF-10A cell line and performed experiments similar to those described above. We treated the cells with resistin at concentrations of 12.5 and 25 ng/ml for up to 5 days and observed cellular morphology. Three days after treatment with resistin at concentration of 25 ng/ml, the cell morphology was transformed into spindle-like shape, which was especially prominent after 5 days of treatment (Fig. 3A). Results from

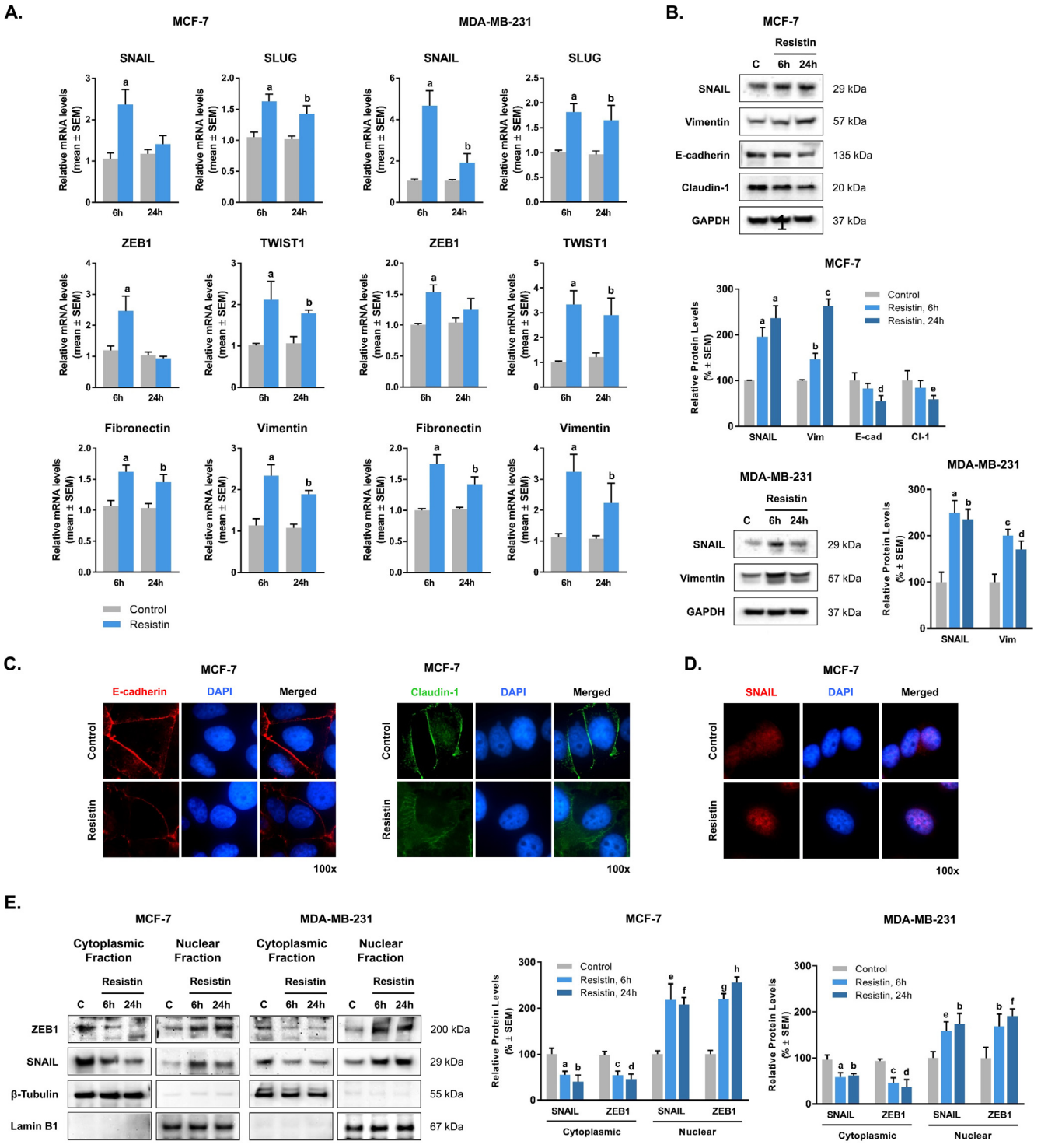

Fig. 2. Resistin induces EMT in breast cancer cells. A. MCF-7 and MDA-MB-231 cells were treated with resistin (12.5 ng/ml) for 6 and 24 h. mRNA expression levels of SNAIL, SLUG, ZEB1, TWIST1, fibronectin, and vimentin were evaluated by qRT-PCR analysis. GAPDH was used as a housekeeping gene. Fold change and *p* values are listed in Supplemental Table 3. B. Western blot and densitometry analyses of MCF-7 and MDA-MB-231 cells treated with resistin (12.5 ng/ml) for 6 and 24 h. Protein levels of SNAIL, vimentin (Vim), E-cadherin (E-cad), and claudin-1 (Cl-1) were evaluated, GAPDH was used as loading control. Densitometry analyses data and *p* values are listed in Table 3 in Ref. [42]. C. Immunofluorescence staining of MCF-7 cells treated with resistin (12.5 ng/ml) for 24 h. E-cadherin and claudin-1 proteins are visualized in red and green, respectively, and nuclei were stained with DAPI (blue). Magnification 100×. D. Immunofluorescence staining for SNAIL protein (red) of MCF-7 cells treated with resistin (12.5 ng/ml) for 24 h. Nuclei were counterstained with DAPI (blue). Magnification 100×. E. Western blot analyses of cytoplasmic and nuclear fractions from MCF-7 and MDA-MB-231 cells blotted for ZEB1 and SNAIL protein. β-Tubulin and Lamin B1 were used as cytoplasmic and nuclear marker, respectively. Bar graphs represent densitometry analyses of the Western blots. Numerical data and *p* values from the densitometry analyses are listed in Table 4 in Ref. [42]. (For interpretation of the references to colour in this figure legend, the reader is referred to the web version of this article.)

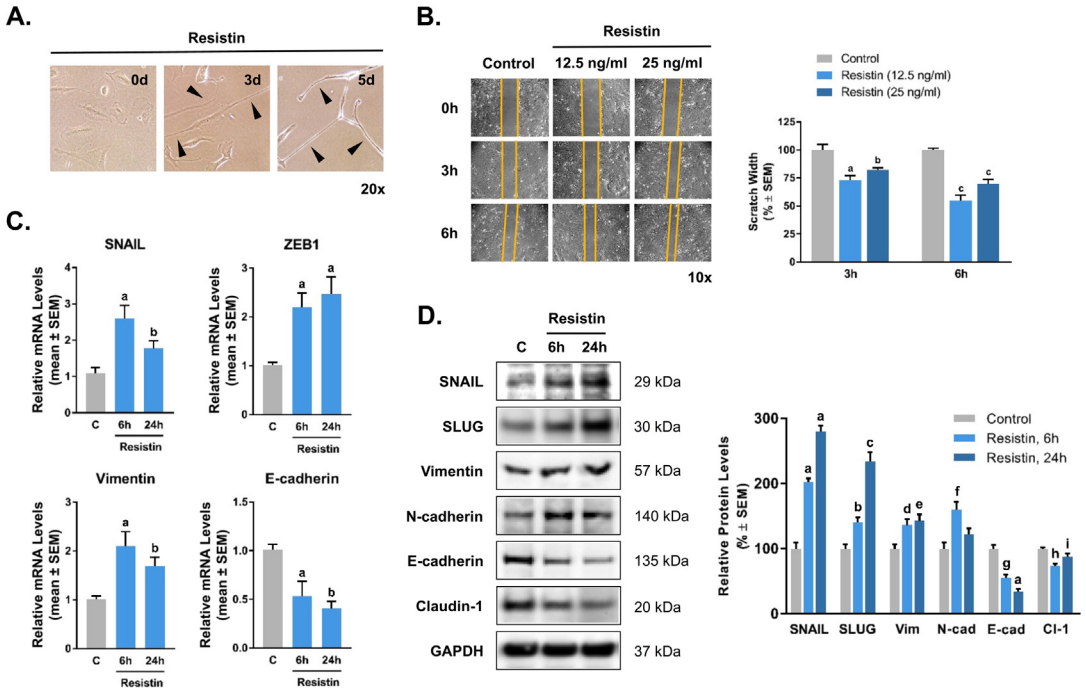

Fig. 3. Resistin induces EMT in breast epithelial MCF-10A cells. A. Cells were treated with resistin (25 ng/ml) for up to 5 days. Phase-contrast images were taken before and 3 and 5 days after treatment. Arrows indicate the formation of cellular protrusions. Magnification 20×. B. Scratch migration wound healing assay of control and resistin-treated cells (concentrations of 12.5 and 25 ng/ml). Phase-contrast images were taken before (0 h) and 3 and 6 h after treatment. Data for cell migration were calculated as fold-change of resistin treatment *vs.* control (non-treatment), as for each scratch the data were normalized to 0 h of treatment. Magnification 20×. Numerical data and *p* values from the scratch migration assay are listed in Supplemental Table 4. C. qRT-PCR analyses of SNAIL, ZEB1, vimentin and E-cadherin mRNA expression. Mean fold change data and *p* values are listed in Supplemental Table 5. D. Western blot analyses of SNAIL, SLUG, vimentin (Vim), N-cadherin (N-cad), E-cadherin (E-cad) and claudin-1 (Cl-1) protein expression. GAPDH was used as a loading control. Bar graph represents data from densitometry analyses of the Western blots. Numerical data from the densitometry analyses and the *p* values are listed in Supplemental Table 6.

scratch migration wound healing assay where cells were treated with 12.5 and 25 ng/ml of resistin, also demonstrated induction of cellular migration by resistin (Fig. 3B and Supplemental Table 4). Quantitative RT-PCR data revealed increased SNAIL, ZEB1 and vimentin mRNA expression in the resistin-treated cells concomitantly with decreased E-cadherin mRNA levels (Fig. 3C and Supplemental Table 5). Western blot analyses demonstrated upregulated protein expression of SNAIL, SLUG, vimentin and N-cadherin, and downregulated protein expression of E-cadherin and claudin-1 after resistin treatment (Fig. 3D and Supplemental Table 6).

3.5. Effects of resistin on EMT are partially mediated by CAP1

In order to determine whether CAP1 plays a role in mediating the effect of resistin on EMT, we knocked-down the expression of CAP1 in MCF-7 cells by using siRNA gene silencing approach. Control analyses showed that while there was no significant difference between CAP1 mRNA and protein levels in the untransfected, Lipofectamine® RNAiMAX-treated or negative siRNA-transfected cells, CAP1 mRNA and protein expression in CAP1 siRNA-transfected cells was significantly reduced (Fig. 4A and B, and Supplemental Tables 7 and 8). We then investigated whether CAP1 gene silencing in MCF-7 cells can disrupt the effect of resistin on the expression of mesenchymal markers. Quantitative RT-PCR analyses revealed that although resistin significantly upregulated SNAIL, ZEB1 and vimentin mRNA expression, when CAP1 was silenced, these effects were abolished (Fig. 4C and Supplemental Table 9). Western blot analyses also demonstrated complete lack of the resistin effect on CAP1, SNAIL and ZEB1 protein expression after CAP1 siRNA transfection (Fig. 4D and Supplemental Table 10). Additionally, immunofluorescence staining of MCF-7 cells revealed that the suppression of CAP1 expression resulted in decreased resistin-induced nuclear translocation of SNAIL and ZEB1 (Fig. 4E). Results from scratch migration wound healing assay (Fig. 4F and Supplemental Table 11) and Transwell migration assay (Fig. 4G and Supplemental Table 12) demonstrated that inhibition of CAP1 transcription decreased MCF-7 cells migration.

3.6. Resistin induces acquisition of cancer stem cells-like properties in breast cancer cells

We finally treated MCF-7 with resistin (12.5 ng/ml for 6 h) in the absence or presence of CAP1 siRNA and performed a quantitative PCR array in MCF-7 cells, profiling the expression of 84 genes related to CSC, pluripotency and metastasis (Fig. 5 and Supplemental Table 13). The results from the array indicated that resistin upregulated the expression of various genes used as CSC markers or involved in cellular proliferation or loss of stemness (Supplemental Table 14). Among these genes, we selected 9 which were either upregulated (ALDH1A1, ITGA4, LIN28B, SMO, KLF17, PTPRC, PROM1) or downregulated (SIRT1, PECAM1) more than 2-fold when the cells were treated with resistin (Fig. 5A–C).

Based on these findings we performed qRT-PCR analyses for the expression of ALDH1, SMO, PROM1, PTPRC, ITGA4, KLF17, SIRT1, and PECAM1. Results from the analysis confirmed the PCR array data and demonstrated that the effect of resistin on PROM1, PTPRC, KLF17, SIRT1, and PECAM1 gene expression was abolished when CAP1 was knocked down (Fig. 5D and Supplemental Table 15).

4. Discussion

In this study, we investigated the *in vitro* effects of the WAT adipokine resistin and the involvement of CAP1 in EMT and stemness in breast cancer cells. As a model we used MCF-7 cells (non-invasive cancer cell line, normally considered to have low metastatic potential),

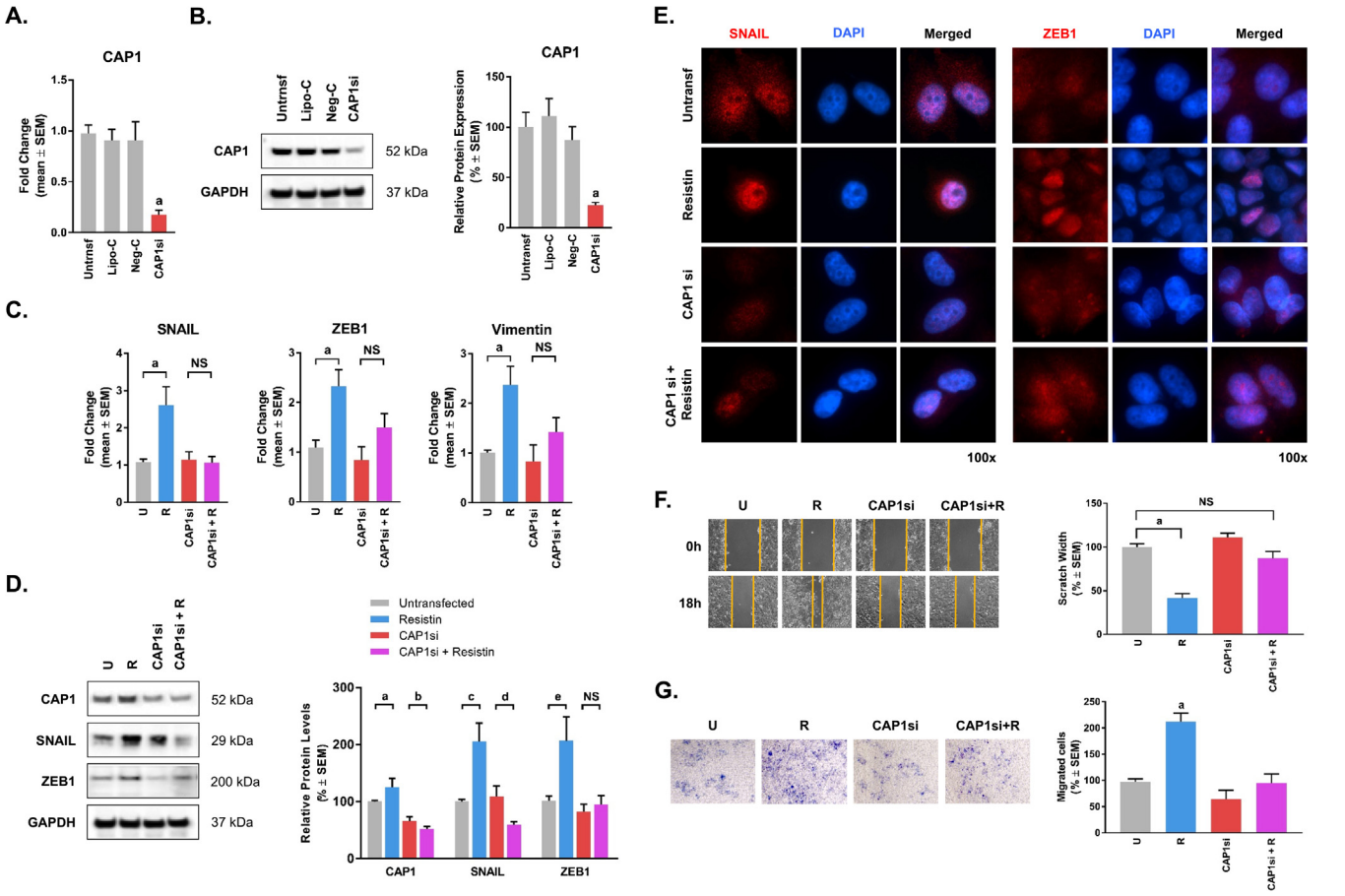

Fig. 4. The effect of resistin on EMT in MCF-7 cells partially depends on CAP1. A and C. Knock-down of CAP1 by using siRNA approach. A. qRT-PCR (GAPDH was used as a house-keeping gene). Abbreviations: Untrnsf, untransfected; Lipo-C, Lipofectamine® control; Neg-C, negative siRNA-transfected; CAP1si, CAP1 siRNA-transfected cells. B. Western blot and densitometry analyses (GAPDH was used as loading control). All numerical data and *p* values from A and B are listed in Supplemental Tables 7 and 8. C. qRT-PCR analyses of SNAIL, ZEB1 and vimentin mRNA expression. SNAIL, ZEB1, and vimentin. Fold change data and *p* values are listed in Supplemental Table 9. NS, non-significant difference. D. Western blot and densitometry analyses for CAP1, SNAIL and ZEB1 protein expression. GAPDH was used as loading control. Numerical and *p* values from the densitometry analysis are listed in Supplemental Table 10. E. Immunofluorescence staining for SNAIL and ZEB1 proteins of untransfected (Untransf), resistin-treated (12.5 ng/ml for 6 h) and CAP1 siRNA-transfected cells, un-treated or treated with resistin. F. Scratch migration wound healing assay of untransfected or CAP1 siRNA-transfected MCF-7 untreated or treated with resistin (12.5 ng/ml for 6 h). Bar graph shows scratch width represented as % difference compared to control. G. Representative images of MCF-7 cells subjected to Transwell migration assay. Bar graph shows migrated cells through the Boyden chamber represented as % compared to control. Numerical and *p* values from F and G are listed in Supplemental Tables 11 and 12.

MDA-MB-231 cells (poorly differentiated, highly invasive cancer cell line), and MCF-10A cells (non-tumorigenic breast epithelial cells line). Our results demonstrated that resistin increased breast cancer cellular migration through cytoskeletal reorganization and induced EMT re-programming and acquisition of CSC-like properties. We were also able to induce mesenchymal reprogramming in non-carcinogenic breast epithelial MCF-10A cells by treating these cells with resistin, thus providing additional evidence for the resistin effects on breast cells motility.

Our initial experiments aiming to optimize the appropriate treatment conditions showed that maximum effect of resistin on the induction of SOCS3 mRNA levels in MCF-7 and MDA-MB-231 cells was reached at concentration of 12.5 ng/ml. Interestingly, in MCF-10A cells, the maximal effects of resistin on cellular migration and induction of mesenchymal markers expression were reached at concentration of 25 ng/ml. Previous *in vitro* studies with various cell culture systems were performed using concentrations of resistin ranging from 1 to 150 ng/ml [43–48].

Our experimental data demonstrated that resistin increased breast cancer cellular motility through reorganization of the F-actin structural proteins inducting EMT reprogramming. EMT is a fundamental process involved in cancer metastasis which enables immobile cancer cells bearing epithelial characteristic and apical-basal polarity to acquire mesenchymal features which promote the development of motile and invasive properties. We also demonstrated that the effect of resistin on EMT is at least partially dependent on CAP1. Silencing CAP1 in MCF-7 cells inhibiteded mesenchymal markers expression, decreased nuclear translocation of EMT transcription factors, and reduced resistin-induced cellular migration and invasion. Importantly, CAP1 may function differently in breast cancer cells with different metastatic potential, which was demonstrated by Zhang and Zhou [49]. In these experiments, CAP1 silencing resulted in inhibition of breast cancer cell invasion in the non-metastatic MCF-7 cells, but increasing the invasion in the metastatic BT-549 cells.

EMT process results in formation of subpopulation of cancer cells with stem-like properties (CSCs). These cells have the ability of self-renewal and are resistant to the conventional chemotherapy. Classically, CSCs are characterized by high expression of cell surface CD44 antigen and low expression or lack of expression of CD24 ($CD44^{+}/CD24^{-/low}$). Additional characteristic of the CSCs is the expression of the so-called Yamanaka factors (OCT4, SOX2, KLF4, and c-Myc) [50] as well as other markers. Previous research [30] found that resistin increases the proportion of $CD44^{high}/CD24^{-/low}$ cells in MCF-7 and T47D breast cancer cell lines. In this study, we used quantitative

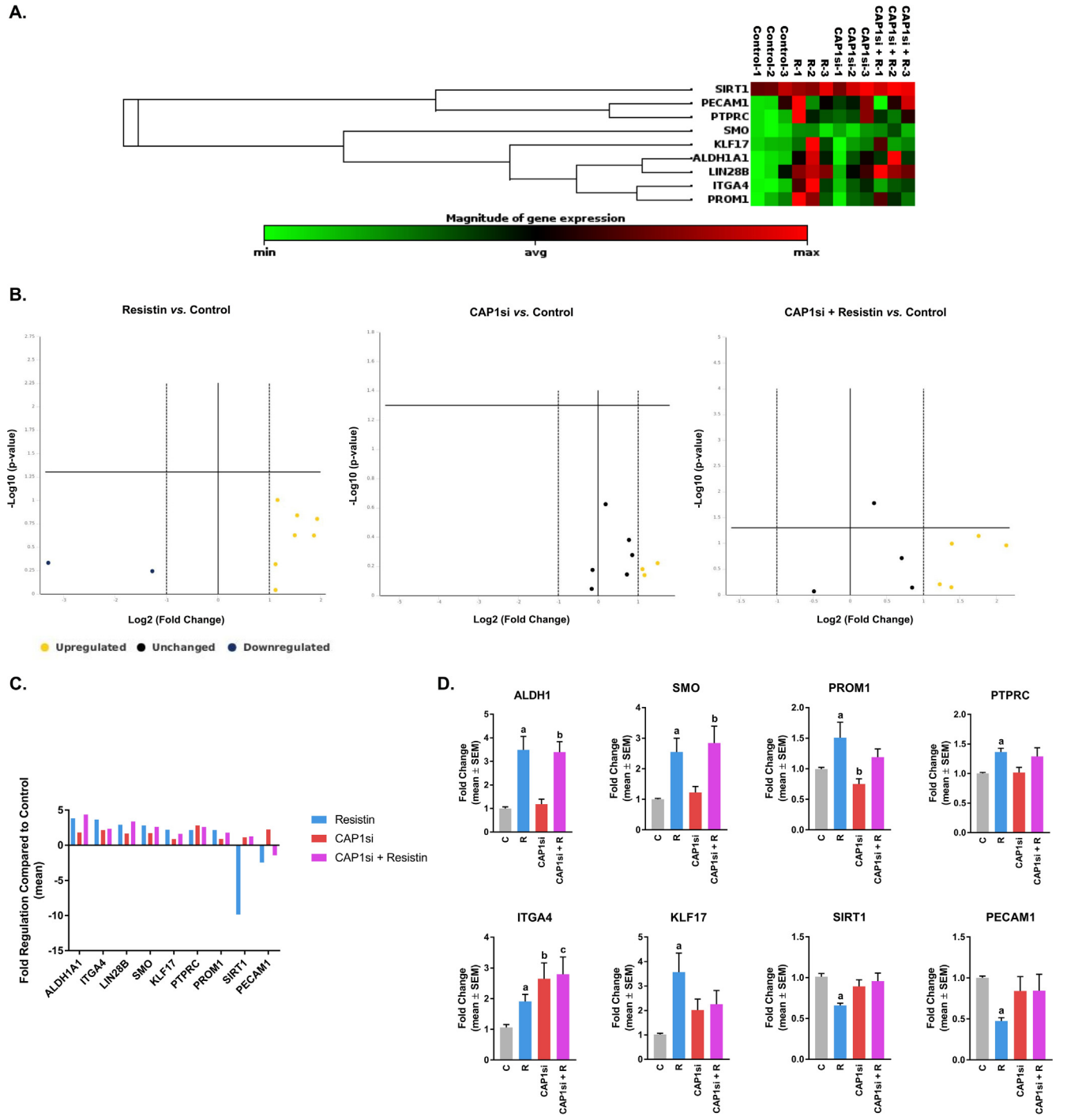

Fig. 5. Resistin modulates CSC reprograming in MCF-7 cells, dependent or independent of CAP1. Results from PCR array for CSC markers (A–D). A. Heat map for selected genes up- or downregulated more than 2-folds by resistin. B and C. Volcano plots and bar graph representing fold-change gene expression after treatment. D. qRT-PCR data for selected gene expression (ALDH1, SMO, PROM1, PTPRC, ITGA4, KLF17, SIRT1, and PECAM1). Fold-change data and *p* values are listed in Supplemental Table 15.

PCR array to profile the expression of 84 genes regulating CSC proliferation, self-renewal, and pluripotency, including genes involved in CSC asymmetric cell division, migration and metastasis as well as genes playing key roles in relevant signal transduction pathways. The data obtained from the PCR array followed by qRT-PCR analyses demonstrated that resistin induced the expression of genes regulating cellular migration and metastasis (KLF17), CSC markers (ALDH1A1, ITGA4, PTPRC, and PROM1) and Hedgehog signaling (SMO) concomitantly with reducing the expression of genes related to asymmetric division (SIRT1) and loss of stemness (PECAM1). These results also showed that the effect of resistin on the expression of some of these genes (KLF17, PROM1, SIRT1, PECAM1) was dependent on CAP1.

Although our study supports the role of CAP1 in mediating resistin-induced EMT and stemness in breast cancer, based on our experimental data we cannot exclude the effect of a possible crosstalk between CAP1 and c-src signaling thus synergizing the resistin actions on EMT. Another weakness of our study stems from the fact that our data were obtained entirely through *in vitro* experimentation. Although we utilized two commonly used breast cancer cell lines, MCF-7 and MDA-MB-231, as well as non-carcinogenic breast epithelial MCF-10A cells, our

findings need to be confirmed in *in vivo* models of breast cancer and in observational studies with human subjects. In a recently published paper [30], resistin was found to increase tumor growth and metastasis in zebrafish and nude mice.

Taken together, our results support the hypothesis that resistin promotes breast cancer progression by inducing EMT reprogramming and acquisition of CSC-like properties in breast cancer cells, and that these effects can be either dependent or independent of CAP1.

5. Conclusions

In conclusion, our study demonstrates that resistin promotes the metastatic potential of breast cancer cells by inducing EMT and stemness and these effects are at least partially mediated by CAP1. Further research is needed to establish a complete signaling pathway(s) and individual molecular players which can be used as potential markers for stratifying specific groups of breast cancer patients for early diagnosis or as novel targets for breast cancer metastasis treatment.

Author's contributions

Dimiter Avtanski conceived and designed the study, participated in data acquisition, performed data analyses, interpreted the data and drafted the manuscript. Anabel Garcia, Beatriz Caraballo, Priyanthan Thangeswaran, Sela Marin, Julianna Bianco and Aaron Lavi participated in data acquisition. Leonid Poretsky critically revised the manuscript.

Declaration of interests

The authors declared that there is no conflict of interest.

Acknowledgment

Funding was provided by Gerald J. and Dorothy R. Friedman New York Foundation for Medical Research.

Appendix A. Supplementary material

Supplementary data to this article can be found online at https://doi.org/10.1016/j.cyto.2019.04.016.

References

[1] Z. Huang, S.E. Hankinson, G.A. Colditz, M.J. Stampfer, D.J. Hunter, J.E. Manson, et al., Dual effects of weight and weight gain on breast cancer risk, JAMA 278 (17) (1997) 1407–1411.
[2] A.G. Renehan, M. Tyson, M. Egger, R.F. Heller, M. Zwahlen, Body-mass index and incidence of cancer: a systematic review and meta-analysis of prospective observational studies, Lancet (London, England) 371 (9612) (2008 Feb 16) 569–578.
[3] K. Bhaskaran, I. Douglas, H. Forbes, I. Dos-Santos-Silva, D.A. Leon, L. Smeeth, Body-mass index and risk of 22 specific cancers: a population-based cohort study of 5·24 million UK adults, Lancet (London, England) 384 (9945) (2014 Aug 30) 755–765.
[4] M.P. Humphries, V.C. Jordan, V. Speirs, Obesity and male breast cancer: provocative parallels? BMC Med. 4 (13) (2015 Jun) 134.
[5] World Health Organization, Obesity and overweight, < http://www.who.int/mediacentre/factsheets/fs311/en/ > (accessed 13 July 2018).
[6] American Cancer Society, Breast Cancer Facts & Figures 2011-2012, American Cancer Society, Inc., Atlanta. < https://www.cancer.org/content/dam/cancer-org/research/cancerfacts-and-statistics/breast-cancer-facts-and-figures/breast-cancer-facts-and-figures-2011-2012.pdf > (accessed 13 July 2018).
[7] S. Cowen, S.L. McLaughlin, G. Hobbs, J. Coad, K.H. Martin, I.M. Olfert, et al., High-fat, high-calorie diet enhances mammary carcinogenesis and local inflammation in MMTV-PyMT mouse model of breast cancer, Cancers (Basel) 7 (3) (2015 Jun 26) 1125–1142.
[8] M.-J. Wu, C.-J. Chang, High fat diet-induced breast cancer model in rat, Bio-protocol 6 (13) (2016).
[9] K.N. Phoenix, F. Vumbaca, M.M. Fox, R. Evans, K.P. Claffey, Dietary energy availability affects primary and metastatic breast cancer and metformin efficacy, Breast Cancer Res Treat. 123 (2) (2010 Sep) 333–344.
[10] A.R. Carmichael, Obesity as a risk factor for development and poor prognosis of breast cancer, BJOG: An Int. J. Obstet. Gynaecol. 113 (2006) 1160–1166.
[11] D.P. Rose, L. Vona-Davis, Interaction between menopausal status and obesity in affecting breast cancer risk, Maturitas 66 (2010) 33–38.
[12] I. Fabregat, A. Malfettone, J. Soukupova, New insights into the crossroads between EMT and stemness in the context of cancer, J. Clin. Med. 5 (3) (2016).
[13] C.M. Steppan, S.T. Bailey, S. Bhat, E.J. Brown, R.R. Banerjee, C.M. Wright, et al., The hormone resistin links obesity to diabetes, Nature 409 (6818) (2001) 307–312.
[14] Siz Zaidi, Tak Shirwany, Relationship of serum resistin with insulin resistance and obesity, J. Ayub Med. Coll. Abbottabad 27 (3) (2015) 552–555.
[15] J. Zhang, Y. Qin, X. Zheng, J. Qiu, L. Gong, H. Mao, et al., The relationship between human serum resistin level and body fat content, plasma glucose as well as blood pressure, Zhonghua Yi Xue Za Zhi 82 (23) (2002 Dec 10) 1609–1612.
[16] K. Azuma, F. Katsukawa, S. Oguchi, M. Murata, H. Yamazaki, A. Shimada, et al., Correlation between serum resistin level and adiposity in obese individuals, Obes Res. 11 (8) (2003 Aug) 997–1001.
[17] M. Degawa-Yamauchi, J.E. Bovenkerk, B.E. Juliar, W. Watson, K. Kerr, R. Jones, et al., Serum resistin (FIZZ3) protein is increased in obese humans, J. Clin. Endocrinol. Metab. 88 (11) (2003 Nov) 5452–5455.
[18] B. Vozarova de Courten, M. Degawa-Yamauchi, R.V. Considine, P.A. Tataranni, High serum resistin is associated with an increase in adiposity but not a worsening of insulin resistance in Pima Indians, Diabetes 53 (5) (2004 May) 1279–1284.
[19] A. Schäffler, C. Büchler, U. Müller-Ladner, H. Herfarth, A. Ehling, G. Paul, et al., Identification of variables influencing resistin serum levels in patients with type 1 and type 2 diabetes mellitus, Horm. Metab. Res. 36 (10) (2004 Oct) 702–707.
[20] A.Z. Jamurtas, A. Stavropoulos-Kalinoglou, S. Koutsias, Y. Koutedakis, I. Fatouros, Adiponectin, resistin, and visfatin in childhood obesity and exercise, Pediatr. Exerc. Sci. 27 (4) (2015 Nov) 454–462.
[21] I. Marcelino-Rodríguez, D. Almeida Gonzalez, J.J. Alemán-Sánchez, B. Brito Díaz, M.D.C. Rodríguez Pérez, F. Gannar, et al., Inverse association of resistin with physical activity in the general population, PLoS One 12 (8) (2017) e0182493.
[22] J. Vendrell, M. Broch, N. Vilarrasa, A. Molina, J.M. Gómez, C. Gutiérrez, et al., Resistin, adiponectin, ghrelin, leptin, and proinflammatory cytokines: relationships in obesity, Obes. Res. 12 (6) (2004 Jun) 962–971.
[23] J.H. Lee, J.W. Bullen, V.L. Stoyneva, C.S. Mantzoros, Circulating resistin in lean, obese, and insulin-resistant mouse models: lack of association with insulinemia and glycemia, Am. J. Physiol. Endocrinol. Metab. 288 (3) (2005 Mar) E625–E632.
[24] Y. Gui, Q. Pan, X. Chen, S. Xu, X. Luo, L. Chen, The association between obesity related adipokines and risk of breast cancer: a meta-analysis, Oncotarget 8 (43) (2017 Sep 26) 75389–75399.
[25] M. Dalamaga, G. Sotiropoulos, K. Karmaniolas, N. Pelekanos, E. Papadavid, A. Lekka, Serum resistin: a biomarker of breast cancer in postmenopausal women? Association with clinicopathological characteristics, tumor markers, inflammatory and metabolic parameters, Clin. Biochem. 46 (7–8) (2013 May) 584–590.
[26] M. Zhang, L. Yan, G.-J. Wang, R. Jin, Resistin effects on pancreatic cancer progression and chemoresistance are mediated through its receptors CAP1 and TLR4, J. Cell Physiol. 14 (2018 Oct).
[27] M. Dalamaga, Resistin as a biomarker linking obesity and inflammation to cancer: potential clinical perspectives, Biomark. Med. 8 (1) (2014) 107–118.
[28] J.O. Lee, N. Kim, H.J. Lee, Y.W. Lee, S.J. Kim, S.H. Park, et al., Resistin, a fat-derived secretory factor, promotes metastasis of MDA-MB-231 human breast cancer cells through ERM activation, Sci. Rep. 5 (6) (2016 Jan) 18923.
[29] S.K. Deshmukh, S.K. Srivastava, H. Zubair, A. Bhardwaj, N. Tyagi, A. Al-Ghadhban, et al., Resistin potentiates chemoresistance and stemness of breast cancer cells: implications for racially disparate therapeutic outcomes, Cancer Lett. 396 (2017) 21–29.
[30] C.-H. Wang, P.-J. Wang, Y.-C. Hsieh, S. Lo, Y.-C. Lee, Y.-C. Chen, et al., Resistin facilitates breast cancer progression via TLR4-mediated induction of mesenchymal phenotypes and stemness properties, Oncogene 37 (5) (2018 Feb 1) 589–600.
[31] Sahmin Lee, Hyun-Chae Lee, Yoo-Wook Kwon, Youngjin Cho, Sang Eun Lee, Han-Mo Yang, Ju-Young Kim, Hyun-Jai Cho, Byung-Hee Oh, Young-Bae Park, H.-S. Kim, Abstract 13041: identification of a human resistin receptor that mediates inflammatory actions, Circulation 126 (Suppl 21) (2012).
[32] S. Lee, H.-C. Lee, Y.-W. Kwon, S.E. Lee, Y. Cho, J. Kim, et al., Adenylyl cyclase-associated protein 1 is a receptor for human resistin and mediates inflammatory actions of human monocytes, CellMetabolism 19 (3) (2014 Mar 4) 484–497.
[33] J. Field, J. Nikawa, D. Broek, B. MacDonald, L. Rodgers, I.A. Wilson, et al., Purification of a RAS-responsive adenylyl cyclase complex from Saccharomyces cerevisiae by use of an epitope addition method, Mol. Cell Biol. 8 (5) (1988 May) 2159–2165.
[34] A.V. Hubberstey, E.P. Mottillo, Cyclase-associated proteins: CAPacity for linking signal transduction and actin polymerization, FASEB J. 16 (6) (2002 Apr) 487–499.
[35] G.V. Kakurina, E.S. Kolegova, I.V. Kondakova, Adenylyl cyclase-associated protein 1: structure, regulation, and participation in cellular processes, Biochemistry (Mosc) 83 (1) (2018 Jan) 45–53.
[36] D. Ksiazek, H. Brandstetter, L. Israel, G.P. Bourenkov, G. Katchalova, K.-P. Janssen, et al., Structure of the N-terminal domain of the adenylyl cyclase-associated protein (CAP) from Dictyostelium discoideum, Structure 11 (9) (2003 Sep) 1171–1178.
[37] S. Ono, The role of cyclase-associated protein in regulating actin filament dynamics – more than a monomer-sequestration factor, J. Cell Sci. 126 (Pt 15) (2013 Aug 1) 3249–3258.
[38] E. Bertling, P. Hotulainen, P.K. Mattila, T. Matilainen, M. Salminen, P. Lappalainen, Cyclase-associated protein 1 (CAP1) promotes cofilin-induced actin dynamics in mammalian nonmuscle cells, Mol. Biol. Cell 15 (5) (2004 May) 2324–2334.
[39] G.-L. Zhou, H. Zhang, J. Field, Mammalian CAP (Cyclase-associated protein) in the world of cell migration: roles in actin filament dynamics and beyond, CellAdh Migr. 8 (1) (2014) 55–59.
[40] Y. Liu, X. Cui, B. Hu, C. Lu, X. Huang, J. Cai, et al., Upregulated expression of CAP1

is associated with tumor migration and metastasis in hepatocellular carcinoma, Pathol. Res. Pract. 210 (3) (2014 Mar) 169–175.
[41] A. Muñoz-Palomeque, M.A. Guerrero-Ramirez, L.A. Rubio-Chavez, R.C. Rosales-Gomez, M.G. Lopez-Cardona, V.H. Barajas-Avila, et al., Association of RETN and CAP1 SNPs, expression and serum resistin levels with breast cancer in Mexican women, Genet. Test Mol. Biomarkers (2018 Mar 20).
[42] D. Avtanski, A. Garcia, B. Caraballo, P. Thangeswaran, S. Marin, J. Bianco, A. Lavi, L. Poretsky, In vitro effects of resistin on epithelial to mesenchymal transition (EMT) in breast cancer cells, Data in Brief (submitted).
[43] A. Rak, E. Drwal, A. Wróbel, E.Ł. Gregoraszczuk, Resistin is a survival factor for porcine ovarian follicular cells, Reproduction 150 (4) (2015 Oct) 343–355.
[44] M. Reverchon, M. Cornuau, C. Ramé, F. Guerif, D. Royère, J. Dupont, Resistin decreases insulin-like growth factor I-induced steroid production and insulin-like growth factor I receptor signaling in human granulosa cells, Fertil. Steril. 100 (1) (2013 Jul) 247-55-3.
[45] M.C. Zuniga, G. Raghuraman, W. Zhou, Physiologic levels of resistin induce a shift from proliferation to apoptosis in macrophage and VSMC co-culture, Surgery 163 (4) (2018 Apr) 906–911.
[46] L. Pang, Y. Zhang, Y. Yu, S. Zhang, Resistin promotes the expression of vascular endothelial growth factor in ovary carcinoma cells, Int. J. Mol. Sci. 14 (5) (2013 May 7) 9751–9766.
[47] M.S. Jamaluddin, S. Yan, J. Lü, Z. Liang, Q. Yao, C. Chen, Resistin increases monolayer permeability of human coronary artery endothelial cells, PLoS One 8 (12) (2013) e84576.
[48] N. Chen, L. Zhou, Z. Zhang, J. Xu, Z. Wan, L. Qin, Resistin induces lipolysis and suppresses adiponectin secretion in cultured human visceral adipose tissue, Regul. Pept. 194–195 (2014 Nov) 49–54.
[49] H. Zhang, G.-L. Zhou, CAP1 (Cyclase-Associated Protein 1) exerts distinct functions in the proliferation and metastatic potential of breast cancer cells mediated by ERK, Sci. Rep. 6 (2016) 25933.
[50] K. Takahashi, S. Yamanaka, Induction of pluripotent stem cells from mouse embryonic and adult fibroblast cultures by defined factors, Cell 126 (4) (2006 Aug 25) 663–676.